

Local-environment effect on the nitrogen bound state in $\text{GaP}_x\text{As}_{1-x}$ alloys: Experiments and coherent-potential approximation theory

H. Mariette

Laboratoire de Physique des Solides, CNRS, 1 place A. Briand, 92190 Meudon-Bellevue, France
and Max-Planck-Institut für Festkörperforschung, 7 Stuttgart 80, Federal Republic of Germany*

J. Chevallier

Laboratoire de Physique des Solides, CNRS, 1 place A. Briand, 92190 Meudon-Bellevue, France

P. Leroux-Hugon

*Laboratoire de Physique des Solides, CNRS, 1 place A. Briand, 92190 Meudon-Bellevue, France
and Groupe de Physique des Solides de l'Ecole Normale Supérieure,* Université Paris VII, Place Jussieu, 75221 Paris Cedex 05, France*

(Received 9 July 1979; revised manuscript received 19 February 1980)

In $\text{GaP}_x\text{As}_{1-x}\text{:N}$ alloys ($0.6 \leq x \leq 1$) the luminescence due to the radiative recombination of nitrogen bound excitons (N_x) is shifted toward lower energies with respect to excitation spectra (A). This shift is attributed to the band broadening generated by local disorder around nitrogen atoms. The broadening and the shift-composition dependences are characterized by their appearance even for very low As concentration and their saturation for $x < 0.8$. The temperature dependence of the luminescence and excitation lines is consistent with a model which we suggest and according to which the luminescence band is generated by the radiative recombination of nitrogen bound excitons which have thermalized toward the bottom of the excitation band broadened by alloy disorder, i.e., by the occurrence of different local configurations As-P around nitrogen atoms. Theoretically, we stress the importance of taking into account the perturbation of the electronic structure brought about by the alloy disorder; to this end we use the coherent-potential approximation (CPA). We find a good agreement with the experimental bowing parameter of the band edges. By using an extension of the CPA incorporating the local environment effect, we account for the evolution of the bandwidth, energy positions, and cross sections of the excitation band (A) versus the alloy composition.

I. INTRODUCTION

Interest in luminescence of nitrogen bound excitons in $\text{GaP}_x\text{As}_{1-x}$ alloys stems from the particular band structure of these alloys which leads to a luminescence cross-section enhancement near the crossing of the X and Γ conduction-band minima about $x = 0.5$.¹ In a previous paper² we showed that the radiative lifetime τ_R of excitons bound to nitrogen atoms depends on the alloy composition for $x > 0.6$: the radiative recombination probability increases as the Γ conduction-band minimum becomes closer to the X conduction-band minimum (this is so-called band-structure enhancement). Recently, two of us,³ by combining excitation and luminescence spectroscopy measurements have shown that, in $\text{GaP}_x\text{As}_{1-x}$ alloys, the excitation line associated with the N bound exciton ground state was broadened and that the luminescence line was shifted to lower energies with respect to the excitation line. The line broadening was attributed to an alloying effect (i.e., disorder arising from different As and P neighbor configurations around a given N center). In this paper we shall develop our interpretation concerning the broadening and the shift effects related to the nitrogen bound-ex-

citon lines. The first step of this analysis consists in subtracting from the experimental spectra the optical- and acoustical-phonon contributions as suggested by Wolford *et al.* in luminescence.⁴ By using this procedure, distinct zero-phonon lines appear both in luminescence and in excitation. We would like to emphasize that this distinction is not generated, as proposed by several authors,^{5,6} by a Frank-Condon mechanism—i.e., by a local lattice distortion around a nitrogen center after trapping of an exciton. We think that this distinction is a consequence of the alloying effect, i.e., of the mechanism responsible for the broadening of the excitation and luminescence lines into bands. While the excitation band reflects the excitonic density of states associated to the different local configurations As-P in the alloy, the luminescence band incorporates the exciton transfer mechanisms towards the low-energy configurations. This transfer mechanism is responsible for the shift between the zero-phonon luminescence and excitation bands. Our interpretations are based upon considerations on alloys very close to GaP.

In their theoretical interpretations, most of the authors⁷⁻⁹ estimate that the singularity of the GaAsP:N system in comparison with GaP:N comes

from the more or less extended tail of the localized potential due to the nitrogen impurity. By focusing their attention on these tails, the previous works used the virtual-crystal approximation (VCA) for describing the host crystal and consequently neglected the specific effects of local disorder on the electronic structure in the alloy. In order to take into account this local environment effect, one needs an adequate theoretical description such as the one provided by the coherent-potential approximation (CPA). We shall show that disorder cannot be neglected in the interpretation of optical experimental data in alloys and explains the observed band broadenings. Without underestimating the importance of problems due to the potential tails which account for a second bound state in the crossover composition region, we shall limit ourselves to the theoretical investigation of these alloying effects developed in the single site CPA.

In the first part of this paper, we shall provide and discuss our experimental data, mainly the influence of the alloy composition ($0.6 \leq x \leq 1$) and of the temperature on the luminescence and excitation spectra related to the recombination of nitrogen bound excitons. We shall see how this brings new information on the alloying effect in $\text{GaP}_x\text{As}_{1-x}:\text{N}$ alloys.

In the second part, we shall show how the CPA can be used for the electronic-band-structure calculation of $\text{GaP}_x\text{As}_{1-x}$ alloys. We shall develop also this formalism for the calculation of the nitrogen bound-state energy under a single site CPA and an extension of this method will be used in order to take into account the local environment effect As-P around the N atom. Following Chen and Sher,¹⁰ we shall show that this perturbation introduced by alloying accounts for the nonlinear variation of the Γ and X band edges. By applying this CPA method, a good agreement is obtained between experimental and theoretical values: the maximum position of the nitrogen bound-state energy, the radiative lifetime of N bound excitons, and, for the first time, the density-of-states broadening.

II. EXPERIMENTAL RESULTS

$\text{GaP}_x\text{As}_{1-x}$ layers were grown by the conventional vapor-phase epitaxy on (100) GaP substrates. Nitrogen doping was achieved from an additional ammonia partial pressure kept constant for each composition. The expected nitrogen concentration range is 10^{18} – 10^{19} cm^{-3} and the free electron concentration is about 7×10^{15} cm^{-3} at 300 K. The alloy composition was determined from x-ray analysis, electron microprobe analysis, and from the free excitonic gap energy for GaP rich alloys.³ We have investigated layers in the composition

range $0.6 \leq x \leq 1$. The thickness of the homogeneous composition region is 20–30 μm . Sample excitation was provided by the green and blue lines of an Ar^+ laser in photoluminescence measurements and by a tunable dye laser in excitation spectroscopy (light power approximately 1 mW).

Typical photoluminescence and excitation spectra are displayed in Figs. 1–4 for several alloy compositions (in this paper, we shall use, arbitrarily, excitation for absorption and emission for luminescence). The dominant luminescence line N_x is

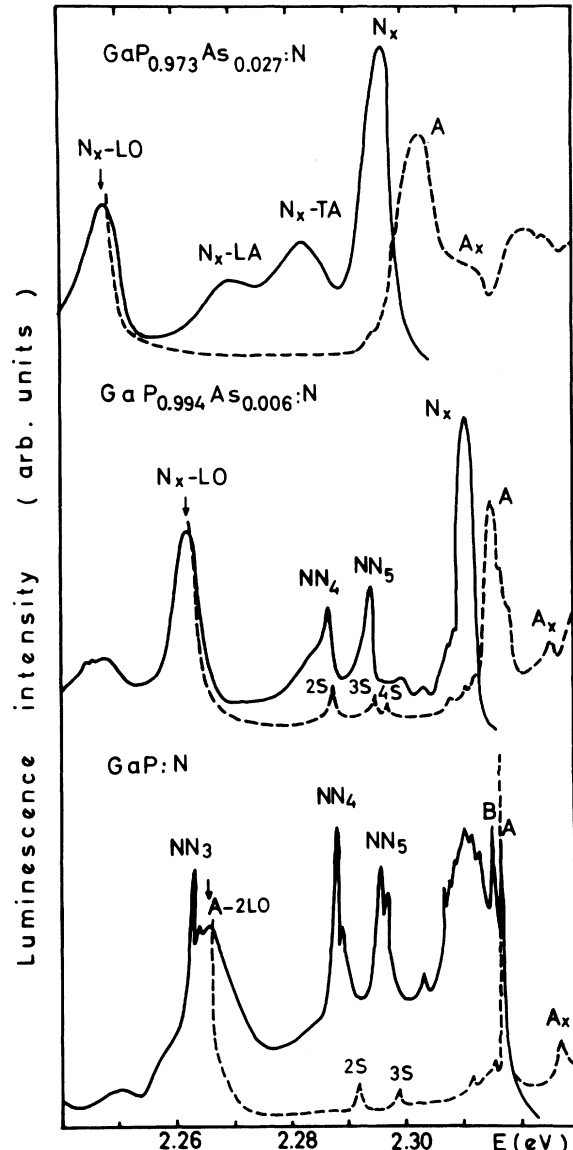


FIG. 1. Typical photoluminescence (continuous line) and excitation spectra (dashed lines) of $\text{GaP}_x\text{As}_{1-x}:\text{N}$ related to the radiative recombination of nitrogen bound excitons for $0.90 < x \leq 1$ at $T=1.6$ K. The figure shows the excitation spectra of the N_x luminescence line—LO-phonon replica.

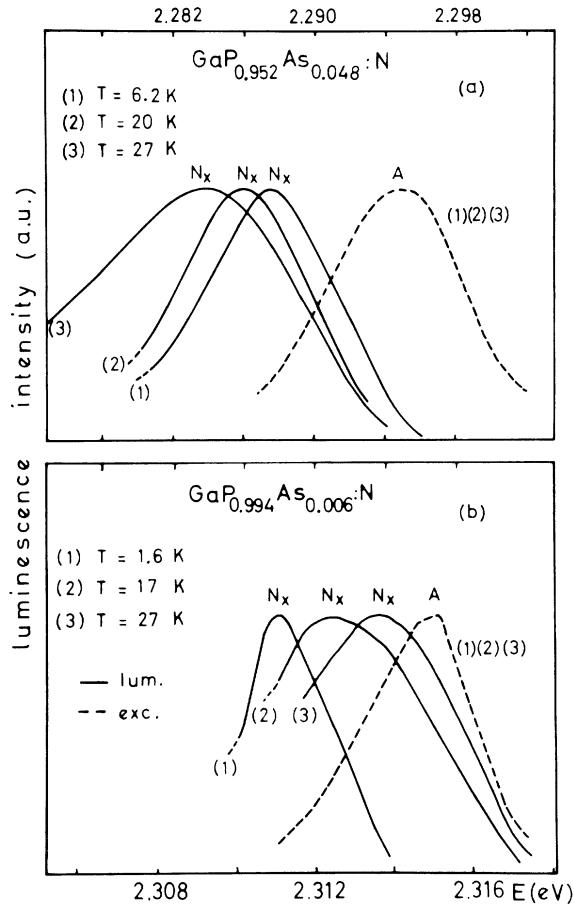


FIG. 2. Temperature dependence of luminescence (N_x) and excitation (A) spectra of two GaP-rich alloys.

attributed to the recombination of excitons bound to isolated nitrogen atoms. This line is always accompanied by several acoustical- and optical-phonon replica. In luminescence excitation spectra, the intensity of the N_x -LO line or N_x line is recorded as a function of the exciting wavelength. Excitation spectra appear similar in both cases above the N_x energy except for the energy position of the usual Stokes lines due to Raman scattering of the laser light (TO and LO phonons).³ However, the excitation spectra of the N_x -LO line provide more information around the N_x line energy because we avoid resonance in this region (Fig. 1). In this paper, we shall emphasize the dominant effect related to the existence and the broadening of the A excitation peak and N_x luminescence peak associated with the N bound-exciton state. We shall detail neither the other features of the excitation spectra (free exciton peak, excited states of NN_3 pairs) nor those of the luminescence spectra (NN_α pairs) because this was presented earlier.^{3,11} As previously noted,³ an increase of the As concentration results not only in a downward shift of both the A

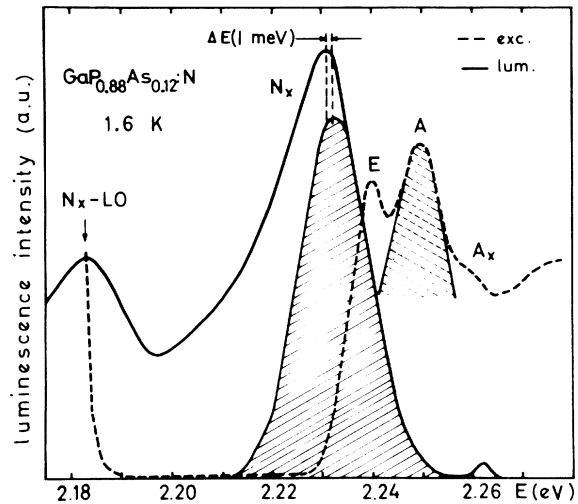


FIG. 3. Typical photoluminescence and excitation spectra for alloys containing 80–90% GaP. The zero-phonon luminescence band (continuous hatching) is deduced from the line-fitting method given in Ref. 12. From this line-fitting we extract a correction ΔE of 1 meV for $x=0.88$. Some uncertainties occur in the bandwidth determination of the zero-phonon excitation band (dashed hatching) because of the presence of the peak E .

and the N_x bands but also in a broadening of the bands and a shift of the N_x band with respect to the A one. Noticeable are the sensitivities of the band broadening and of the energy shift $A - N_x$ to the amount of arsenic in the alloy.

For the sake of clarity, we will discuss first the spectra of GaP-rich samples ($x > 0.90$) and then those of samples with higher GaAs concentration

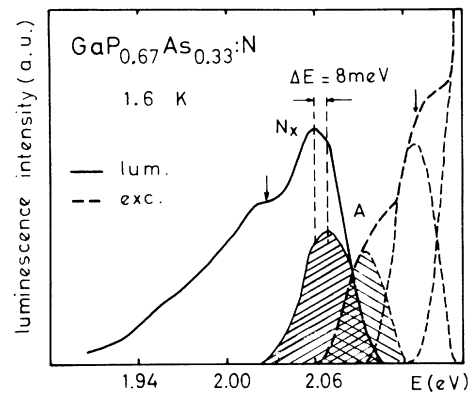


FIG. 4. Typical photoluminescence and excitation spectra for arsenic-rich samples ($0.6 \leq x \leq 0.8$). The zero-phonon luminescence band (continuous hatching) is deduced from the line-fitting method of Ref. 12 and we obtain a correction ΔE of 8 meV for $x=0.67$. The arrows locate the estimated optical-phonon-replica positions. The zero-phonon excitation band (dashed hatching) was deduced after subtracting the optical-phonon contribution and the band-edge absorption.

($0.60 \leq x \leq 0.9$). Such a distinction is necessary because of the drastic shape difference in the various spectra. For $x > 0.90$, the spectra are correctly resolved so that the phonon sidebands cannot be superimposed on the zero-phonon bands and contribute neither to the broadening of the bands nor to a shift of their maxima. On the contrary, in the A and N_x bands of As-rich samples, the TA- and LA-phonon replica do overlap the zero-phonon bands, resulting in an effective bandwidth larger than that of the zero-phonon band and in an energy shift of the band maxima.

A. $x > 0.90$

In this composition range, the luminescence and excitation spectra are clearly resolved and the NN_α structures rapidly vanish as x decreases. For $x = 0.973$ (see Fig. 1) the NN_α lines ($\alpha > 4$) have already disappeared while the LA- and TA-phonon replica rise because of an increase of the Huang-Rhys electron-phonon coupling factor as described by Wolford *et al.*¹² The acoustical-phonon replica do not merge into the A and N_x bands: the relative intensity of these replica with respect to N_x , their energetic position (TA ≈ 12 meV and LA ≈ 25 meV below N_x) and their bandwidths cannot give rise to any energy shift of N_x due to a superimposition of N_x on its LA- and TA-phonon replica. Similarly, the A excitation line is not affected by its phonon replica. As an example, Fig. 1 shows that for $x = 0.994$, the A and N_x bandwidths (respectively, 3 and 2.4 meV) are smaller than the acoustical-phonon energies.

The major results for these samples are the simultaneous appearance of the $A-N_x$ energy shift and of the band broadening as soon as arsenic is added to the binary GaP. Very recently, we have observed this shift even in samples prepared by liquid phase epitaxy and containing around 1‰ arsenic: the $A-N_x$ energy difference was 1 to 2 meV.

In GaP we do not observe any shift between absorption and emission spectra (see Fig. 1), while a shift appears even for a very low amount of arsenic in the host matrix. Such a shift has been attributed to a strong electron-lattice coupling related to a strong localized potential.⁵ In GaP, the potential is not deep enough to generate such a Stokes shift (Fig. 1). We would hardly understand why a Stokes shift would appear for GaP very rich alloys because the nitrogen binding energy and the corresponding potential are approximately constant in this composition range $x > 0.90$. Thus we have interpreted this shift in terms of an alloying effect and not in terms of an electron-lattice coupling. As a consequence, one can define a zero-phonon luminescence line and a zero-phonon excitation

line.

From these remarks, one deduces that for $x > 0.90$ the experimental $A-N_x$ shift is exactly the energy difference between the two zero-phonon bands. A qualitative explanation of this shift can be developed from the existence of local disorder in alloys. The A band is expected to reflect the density of states of N bound states, broadened by the effect of local environment. In other words, the broadening is due to the different configurations As-P surrounding nitrogen atoms in the host matrix. The absorption intensity $I_a(E)$ is the product of this density of states $\rho(E)$ times the cross section $\sigma(E)$. The luminescence line reflects the actual bound-exciton population: it depends on $I_a(E)$ and on the mechanism (e.g., transfer by hopping) responsible for the thermalization of created bound excitons toward the lowest energy states of the A band. This interpretation implies that the ΔA bandwidth and the $A-N_x$ shift have comparable magnitude as experimentally observed (Figs. 5 and 6). In this paper we will not deal with this transfer. Admittedly, this mechanism will be similar to the one which leads to the enhancement of the NN_α lines in the emission spectrum of GaP.¹³ However, our previous qualitative description is supported by temperature-dependent luminescence and excitation measurements. Figure 2 shows that the absorption-band characteristics (peak position, bandwidth) are not sensitive to temperature in the range 1.6–27 K, while the luminescence band broadens when this parameter increases. Such a behavior is expected, respectively, for the density of states and for the bound-exciton population.

B. $x \leq 0.90$

In this case, the experimental results must be carefully interpreted by taking into account the participation of phonons but we shall see that the previous conclusions remain valid. The emission and the absorption bandwidth and the $A-N_x$ energy shift become comparable with typical energies of acoustical or optical phonons. Their quantitative description supposes that we consider the electron-lattice coupling effect.⁴ This correction is also justified because this coupling strength becomes more important in alloys containing more arsenic.¹²

In our luminescence spectra, we take into account the shift of the zero-phonon luminescence line due to its superimposition on the different phonon replica by using the recent linefitting results obtained by Wolford *et al.*⁴ The zero-phonon luminescence line (continuous hatching on Figs. 3 and 4) can be easily deduced. This correction is only 1 meV for $x = 0.88$ and becomes 8 meV for $x = 0.67$.

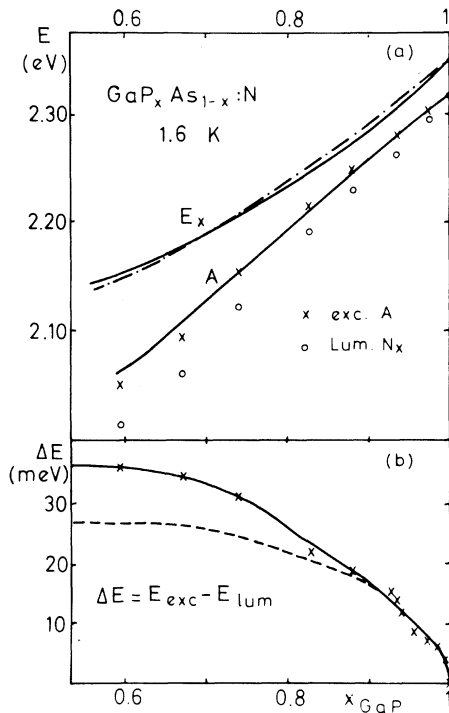


FIG. 5. (a) Composition dependence of the band gap and N bound-state energies. The discontinuous line shows the experimental determination of the E_x indirect band gap energy from Ref. 25 and 26. The two continuous lines are our calculated values of E_x and the nitrogen band state (A) within the coherent-potential approximation. Crosses and dots are respectively our experimental values of excitation and luminescence spectra. (b) Evolution of the experimental energy shift ΔE between excitation and luminescence lines versus composition (continuous line). The dashed line represents the pure energy shift after correction due to the superimposition effect of the zero-phonon band on its phonon replica.

In our excitation experiments, two kinds of spectra have to be considered. For samples with composition $0.8 \leq x \leq 0.9$, excitation spectra similar to Fig. 3 show several features: the free exciton peak (A_x), the nitrogen line (A), and a peak labeled E already reported in Ref. 3. The existence of this last peak brings some inaccuracy into the A bandwidth determination as we report in Fig. 6 for these samples. The peak E could be due to the creation of excitons bound to residual donors (sulphur, tellurium, or selenium) followed by an energy-transfer process towards nitrogen centers. The maximum variation (see Fig. 2 in Ref. 3) and the bandwidth of E vs x are in good agreement with the behavior of excitons bound to shallow donors detected in luminescence.⁴ For arsenic-rich samples ($x < 0.8$) the zero-phonon excitation band is deduced after taking into account the optical-phonon replica (indicated by arrows in Fig. 4). The accuracy of the maximum

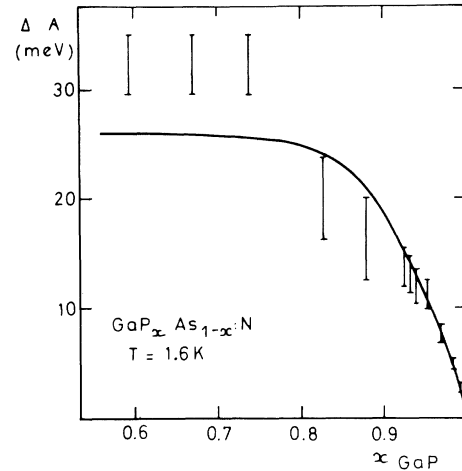


FIG. 6. Experimental points (with error bars) and calculated values (continuous line) of the excitation bandwidth ΔA .

position and the bandwidth is poor for these samples. However, we clearly see in Figs. 5(b) and 6 the saturation effect concerning the evolution of the shift and the band broadening with the composition.

C. Discussion

From the above considerations about the effect of phonons, we are able to deduce in a wide composition range ($0.6 \leq x \leq 1$) the energy-shift value exclusively due to local disorder in alloys [dashed line in Fig. 5(b)] and a good estimation of the zero-phonon excitation bandwidth (ΔA) (Fig. 6). Both quantities are a significant fraction of the N bound-state binding energy and vary with composition in a highly nonlinear way: increasing the As concentration by two orders of magnitude leads only to a tenfold increase of the bandwidth. In our interpretation, contrary to the luminescence band N_x , the zero-phonon excitation band A represents the density of states introduced by nitrogen in these alloys. This means that the intrinsic characteristic of the bound state (density of states) is provided by the absorption band and not by the luminescence band.

We would like now to stress two points. First, we have made clear that the band-broadening effect, which has been observed in a wide variety of materials, is not associated with any chemical fluctuation of composition but results from an alloy disorder due to the local atomic configuration (As or P) surrounding a given Ga site of the lattice; in other words, the band-broadening phenomenon is an intrinsic feature of the alloy as the bowing of the band gap is (see below). Second, because the relative amplitude of the potential fluctuation

tuations and its effect on the bound-state energy decrease when the sampling volume increases, the atomic scale fluctuation of the environment may be experienced only by a local probe such as the N bound exciton which is expected to have a localized wave function, whereas an exciton with a more extended wave function, such as the effective mass exciton, would average out most of the potential fluctuations. This is the reason why, at a given concentration, the band broadening is more important for an N bound exciton than for an exciton bound to a neutral donor such as Se in $\text{GaP}_x\text{As}_{1-x}$ (Ref. 4) or the shallow residual donor in $\text{Ga}_y\text{In}_{1-y}\text{P}$.¹⁴

The discussion given in this section emphasizes the importance of the disorder introduced by the (admittedly) random distribution of As and P atoms and, as a consequence, the necessity to properly incorporate it in the calculations of the electronic structure of the band and of the bound state associated with it. Clearly some approximations are needed and, among the available methods, the so-called coherent-potential approximation (CPA) seems to qualify itself owing to the facts that (i) the disordering potential is expected to have a local (atomic) character, (ii) the method is relatively simple to implement numerically, and (iii) it lends itself (although in a somewhat unsatisfactory way) to include the effect of local configurations (clusters).

III. CPA APPROACH TO THE ELECTRONIC STRUCTURE OF THE $\text{GaP}_x\text{As}_{1-x}$:N ALLOY

Any discussion of the $\text{GaP}_x\text{As}_{1-x}$ luminescence has to take into account the peculiar band structure of this system and its evolution with the alloy composition. To this end, Scifres *et al.*¹⁵ have suggested partitioning the conduction band into three semi-elliptic subbands, centered on the Γ , X , and L points of the Brillouin zone and specified by their half-width W_α , the position of their center V_α , and their contribution P_α to the whole density of states. One then assumes W_α and V_α to vary linearly with composition, the position of the N bound state being calculated within a Koster-Slater approximation. This procedure, which is essentially the virtual-crystal approximation (VCA), neglects any effect specifically associated with the alloy disorder that is with the scattering of electrons on metalloid sites randomly occupied by As or P atoms. The scattering effect modifies the density of states in the bands and thus, through the Koster-Slater method, the electronic structure of the N bound state. In a A_xB_{1-x} alloy, as far as the disorder may be specified by the local values V_A and V_B of potentials on sites A and B , one may account for the effect of disorder within the coherent-potential approximation.¹⁶⁻¹⁸

A. Single-site CPA

In the simplest form of the CPA, the actual alloy is approximated by an effective medium which is made by placing on every site an energy-dependent, complex potential, the self-energy Σ which is chosen in such a way that the scattering produced by one site, on which Σ is replaced by either V_A or V_B , vanishes on the average. Using this formalism for our pseudobinary system and in keeping with its specificity (in particular with the existence of a Γ - X crossing), we will introduce three self-energies Σ_α , corresponding to the three subbands ($\alpha = \Gamma, X, \text{ and } L$), and given by three CPA equations:

$$x \frac{V_\alpha^{(P)} - \Sigma_\alpha}{1 - \Delta V^{(P)}_F} + (1-x) \frac{V_\alpha^{(As)} - \Sigma_\alpha}{1 - \Delta V^{(As)}_F} = 0, \quad (1)$$

where assuming vanishing nondiagonal matrix elements

$$\Delta V^{(P, As)}_F = \sum_{\alpha=\Gamma, X, L} (V_\alpha^{(P, As)} - \Sigma_\alpha) F_\alpha, \quad (2)$$

with

$$F_\alpha(z) = F_\alpha^0(z - \Sigma(z)) = \int \frac{\rho_\alpha^0(E) dE}{z - \Sigma_\alpha(z) - E}, \quad (3)$$

$\rho_\alpha^0(E)$ being the unperturbed (i.e., VCA) partial density of states

$$\rho_\alpha^0(E) = 0 \quad \text{for } |E - V_\alpha| > W_\alpha,$$

$$\rho_\alpha^0(E) = \frac{2P_\alpha}{\pi W_\alpha} [W_\alpha^2 - (E - V_\alpha)^2]^{1/2} \quad \text{for } |E - V_\alpha| \leq W_\alpha.$$

The alloy density of states is then given by

$$\rho(E) = -\frac{1}{\pi} \text{Im}[F(E + i0)] \quad \text{with } F = \sum_{\alpha=\Gamma, X, L} F_\alpha.$$

To get it, at a given value of E , we have to find the self-energies Σ_α which satisfy both Eqs. (1) and (3).

As pointed out by Chen and Sher,¹⁰ the CPA lends itself to calculate the bowing effect, which is the difference between the linearly interpolated variation of the band edge position with the alloy composition and the actual nonlinear variation. Calculation of this bowing effect, specifically due to the alloy disorder, gives us a test of the validity of the alloy electronic structure calculation. The conduction band edge position E_α is obtained from the prescription

$$\lim_{E \rightarrow E_\alpha} \rho(E) \rightarrow 0. \quad (4)$$

It is customarily assumed that in GaP, and in as much as the N_x bound state only is considered, in GaPAs alloys the isoelectronic N atom introduces

only a local potential on the substituted site.²⁹ The condition for a single impurity center to form a bound state at an energy E_N is that the T matrix associated with the impurity site has a pole at $z_N = E_N + i0$, a condition which we will approximate in our (multiband) case by

$$1 - [V_N - \Sigma(z_N)]F(z_N) = 0, \quad (5)$$

with

$$\text{Im}(F(z_N)) = 0,$$

V_N being an average nitrogen potential, and

$$\Sigma(z_N) = \sum_{\alpha=\Gamma, X, L} P_\alpha \Sigma_\alpha(z_N).$$

Note that (5) simply amounts to the one-site Koster-Slater condition, expressed for the effective medium.

Another feature of the N bound state is its optical capture cross section $\sigma(E_N)$ which in a pure crystal is proportional to the square of the $k=0$ component of the wave function (i.e., to the component which corresponds to the direct transition). The cross-section enhancement (band-structure effect) derives from the fact that in the expression of $\phi(k=0)$ (Ref. 19):

$$|\phi(k=0)|^2 = \frac{\Omega}{2\pi^3} \frac{1}{[E_c(k=0) - E_N]^2} \left(\int \frac{\rho(E)dE}{(E - E_N)^2} \right)^{-1} \quad (6)$$

enters an energy denominator proportional to the square of the difference between the bound-state energy and the bottom of the Γ band, $E_\Gamma = E_c(k=0)$. The above formulation is no longer strictly valid for an alloy because, for the dispersion relation $E(k)$, the wave-vector conservation rule does no longer strictly hold. Although the CPA formalism may be used to analyze the optical absorption in an alloy,²⁰ and although the breaking of the k conservation may modify the absorption cross section, we will assume the main effect of alloying to be the change in the energy denominator brought about by composition variation. Thus we still take $\sigma \propto |\phi(k=0)|^2$ with $\phi(k=0)$ given by (6) in which has been introduced the effective medium parameter, namely the self-energy $\Sigma = \Sigma(z = z_N)$, that is the effective potential actually experienced by the bound electron. For semi-elliptic bands (6) may be expressed¹⁹ as

$$|\phi(k=0)|^2 = \frac{B}{(E_\Gamma - E_N)^2} \times \left[\sum_{\alpha=\Gamma, X, L} \frac{P_\alpha}{W_\alpha^2} \left(\frac{\beta_\alpha}{(\beta_\alpha^2 - 1)^{1/2}} - 1 \right) \right]^{-1}, \quad (7)$$

where B is a constant, $E_\Gamma = \Sigma_\Gamma(z_N) - W_\Gamma$, and $\beta_\alpha = [\Sigma_\alpha(z_N) - E_N]/W_\alpha$.

B. Effect of local environment

The local character of the N bound state makes it very sensitive to the local environment, i.e., to the local P and As configuration surrounding a given N impurity. In other words, unlike an effective masslike exciton, the N bound state acts as a local probe of the alloy configuration. There have been numerous attempts²¹⁻²³ to extend the single-site CPA in order to incorporate the effect of configurations, by performing the self-consistent averaging process which defines the effective medium on a distribution of clusters rather than simply on the binary-site distribution. Among these methods, we have chosen the one of Brouers *et al.*²³ which deals with nearest neighbors in a Bethe-Peierls approximation and yields explicit expressions. To calculate the partial contribution F_A and F_B to the Green's function F , Brouers *et al.*²³ do not simply sum terms like F_A :

$$F_A = [1 - (V^{(A)} - \Sigma)F]^{-1}$$

which would lead to the single-site CPA equation (1), but rather they sum terms like $F_A^{(N_A)}$ specified by the nature of the central site and by the number N_A of its nearest neighbor of type A in a given configuration

$$F_A^{(N_A)} = \{z - V^{(A)} - \Delta E^{(N_A)} - [(z - \Sigma)F - 1]F^{-1}\}^{-1}, \quad (8)$$

where enters a renormalization term $\Delta E^{(N_A)}$ which is a function of N_A , of $V^{(A)}$ and $V^{(B)}$, and of Σ and z . If we surround an N impurity by N_A nearest neighbors of type A , there will be a bound state at an energy $E_N^{(N_A)}$ provided that

$$z_N^{(N_A)} - V_N - \Delta E^{(N_A)} - [(z_N^{(N_A)} - \Sigma)F - 1]F^{-1} = 0, \quad (9)$$

with

$$\text{Im}[F(z_N^{(N_A)} + i0)] = 0.$$

This procedure may give as many bound states as there are configurations, namely $Z + 1$, where Z is the number of nearest neighbors. Assuming a random distribution of A and B atoms, the occurrence probability of a given configuration $P^{(N_A)}$ is given by the binomial distribution. Let us notice that, for the sake of simplicity, we have limited ourselves to consider the As-P nearest neighbors only, but that by incorporating successive outer shells of neighbors, we would get a larger number of configurations in such a way that, ultimately, we expect the N bound-state spectrum to be a continuous spectrum rather than a discrete one.

C. Comparison with experiment

We have first studied, using formulas (1) to (4), the composition dependence of the band-edge position. Values of bandwidth W_α , positions V_α , and contributions P_α of each band are given in Table I for GaAs and GaP. The values of P_α which differ from those used by Scifres *et al.*¹⁵ are obtained from the consideration of the Brillouin-zone geometry as discussed in the Appendix. In the alloy we have used a linear interpolation for W_α . As the experiments actually measure the band gaps rather than the absolute band-edge positions, we have also calculated the valence-band-edge variation with composition. This is done within the CPA, assuming a single, semi-elliptic form of the density of states with a constant bandwidth, $W_v = 2$ eV and a 0.1-eV shift of the valence band edge between GaAs and GaP.²⁴ With this model we are able to correctly estimate the bowing of the band gap in the whole concentration range ($0 \leq x \leq 1$) using no input parameters other than the band-structure parameters for GaAs and GaP incorporated in the phenomenological Green's function F_α^0 ; a sensitive check is the concentration x for the crossing of Γ and X minima. As seen in Fig. 7, the calculated crossing composition agrees with experiment.^{25, 26}

From the experimental excitation spectrum, one may deduce the composition dependence of the maximum of the A band, E_A , and its half-bandwidth ΔA . To compare these values to the theory, we have calculated a histogram with 13 points corresponding to the 13 configurations of nearest neighbors P and As around an N center. The abscissas of the histogram are the $E_N^{(NA)}$ which are solutions of Eq. (9), and the ordinates are proportional to the product of the probability $P^{(NA)}$ by the cross-section term $|\phi(k=0)|^2$ given by formula (7) where E_N is replaced by $E_N^{(NA)}$. The calculated values of E_A and of ΔA are then deduced from, respectively,

TABLE I. Parameters used in the calculations: contribution P_α of each band ($\alpha = \Gamma, L, X$) to the whole density of states, effective masses m_α , half-width of the density-of-states band, and center position V_α of each band measured from the valence-band maximum of GaP taken as the origin for the calculations.

		P_α	m_α/m_0	W_α (eV)	V_α (eV)
GaP	Γ	0.0379	0.120	1.3032	4.1872
	X	0.4792	0.760	1.1166	3.4656
	L	0.4829	1.010	1.8444	3.5894
GaAs	Γ	0.0379	0.067	2.1713	3.7903
	X	0.4792	0.850	0.9290	3.0410
	L	0.4829	0.560	1.4171	3.3321

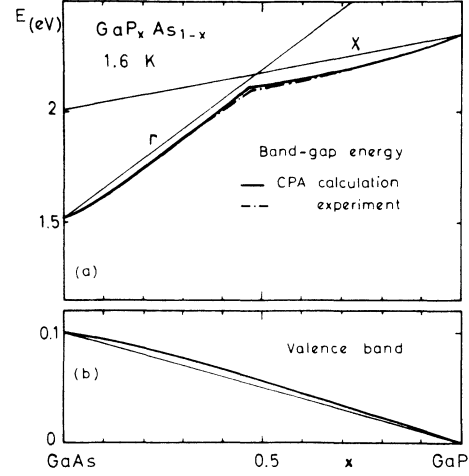


FIG. 7. Calculation of the alloy band structure within the CPA method (heavy line) compared with the linear interpolation provided by the VCA method (narrow line). (a) CPA band-gap energy compared with the experimental data of Refs. 25 and 26 (dashed line). (b) Calculation of the valence-band maximum energy within the CPA (the energy difference between the two extreme binary compounds is given by Ref. 24).

the first and second moments of the histogram. To get $E_N^{(NA)}$, we need the value of the nitrogen potential V_N . Assuming V_N to vary linearly with x , we have adjusted it from the position of the A line in GaP and from the position of the maximum of the A band in $\text{GaP}_{0.74}\text{As}_{0.26}$. As experimentally we are dealing with an exciton bound state rather than an electron bound state, this procedure amounts to taking into account the hole potential in the form of a local potential on the N site. Another procedure is to adjust V_N in order to have $E_A = (E_A)_{\text{expt}} - E_{\text{ex}}$ where $(E_A)_{\text{expt}}$ is the observed energy of the N bound-exciton state and E_{ex} the electron-hole binding energy [an estimate is $E_{\text{ex}} = 11$ meV for GaP (Ref. 27)]. Both procedures give essentially the same results for the variation of ΔA as a function of x . The calculation of the renormalization term $\Delta A^{(NA)}$ involves both the diagonal (in site representation) Green's function $G_{ii} = F$ and the non-diagonal G_{ij} , where i and j are nearest neighbors. In the tight-binding model used in Ref. 23, there is a simple relation between G_{ii} and G_{ij} . This relation is not expected to hold for our pseudobinary system because, in the first place, the unperturbed density of states we start from are not derived from a tight-binding calculation and, in the second place, the As and P are not first but second neighbors. To perform the calculations, we have, however, assumed the relation between G_{ii} and G_{ij} to still hold but with a γ proportionality constant which is adjusted from experiments.

In Fig. 5 we compared the composition depen-

dence of E_A , the maximum of the A band, calculated from the above procedure, and the experimental value obtained from the excitation spectra. There is a good agreement between theory and experiment. Let us point out that, although the variation of E_A with composition does not parallel the variation of the X band edge, the deepening of the N bound state with composition is not as large as was thought before from consideration of the luminescence data; a significant part of this apparent deepening was in fact arising from the shift between excitation and luminescence.

In Fig. 6 we compared the calculated composition dependence of the half-bandwidth ΔA to the value deduced from the excitation spectra.

The ΔA variation is correctly fitted for GaP-rich alloys by setting γ equal to 1.8. This parameter is adjusted in this composition range because the experimental band broadening is not affected by phonons and because the calculated width is very sensitive to γ . For $x < 0.8$ we observe experimentally a saturation effect of the band broadening which is well reproduced by our theory. However, the calculation gives a bandwidth ΔA lower than the experimental value for $x < 0.80$ (Fig. 6). We suggest that the discrepancy comes from an additional band broadening due to acoustical-phonon sidebands (we have been able to evaluate the contribution to the bandwidth only for optical phonons). Our calculations reproduce fairly well the experiments, especially as regards the highly nonlinear variation of ΔA with composition x . This nonlinear behavior is typically what one expects from a CPA-like approach to disorder effect.

At this stage, it may be worth pointing out that the half-width ΔA does not only depend on the alloy composition x and on the potential differences $[V_\alpha^{(P)} - V_\alpha^{(As)}]$ —that is the parameters which appear explicitly in the renormalization energy—but also on the defect potential V_N : at a given composition, a larger potential difference between the impurity and the host matrix, giving rise to a bound state deeper in the gap would lead to a smaller bandwidth. This is not unexpected because, in formula (9), $F(z_{NA}^N)$ depends on V_N . In other words, the relatively large ΔA we have observed is partly due to the fact that the N bound states in GaP and in $\text{GaP}_x\text{As}_{1-x}$ alloys, although localized, turn to be rather shallow states.

Finally, in Fig. 8, we compared the luminescence decay time τ_R , obtained from time-resolved spectra experiments² and the value of $|\phi(k=0)|^2$ calculated for the energy of the emission-band maximum. τ_R is expected to be inversely proportional to $|\phi(k=0)|^2$, the proportionality constant being adjusted from the data on GaP. As seen from Fig. 8 our fit correctly reproduces the rapid decrease

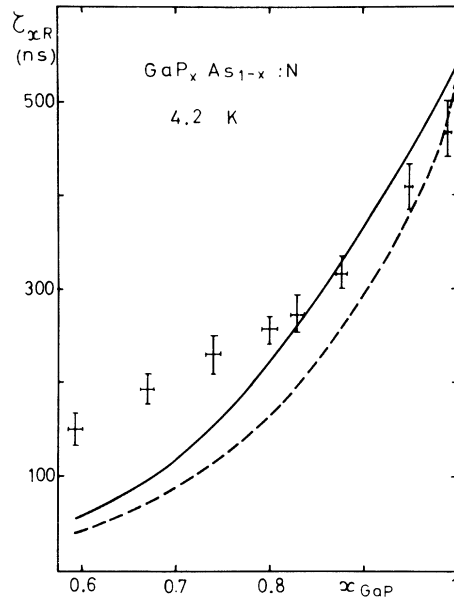


FIG. 8. Variation of the radiative lifetime of the nitrogen bound exciton with alloy composition. The continuous line is the result calculated within the CPA method. The experimental values (+) and results from a more empirical model (dashed line) are taken from Ref. 2.

of τ_R with decreasing composition, that is, the band-structure effect. This agreement ensures us of the validity of the alloy electronic structure calculation which enters the expression of $|\phi(k=0)|^2$ through the density of states and through the Γ band-edge position. It is worth emphasizing that our fit involves no adjustable parameters, unlike previous attempts in the literature, in which, for each composition, the band-edge position had been inferred from experiments. From the calculation we find the general behavior of the experimental curve and particularly the rapid decrease for GaP-rich alloys. However, to ascertain whether this discrepancy between the model and the experiment is an intrinsic weakness of this model would require a more thorough analysis of the relation between τ_R and σ than the one we have performed.

IV. CONCLUSION

The main results of the present paper can be summed up as follows. We have extended our previous experimental results in $\text{GaP}_x\text{As}_{1-x}:\text{N}$ about the broadening of the excitation line, the shift between emission and absorption peaks, and the temperature influence on these effects: The broadening and the shift-composition dependences are characterized by their appearance even for very low As concentration and their saturation for $x < 0.8$. We have shown experimentally that, in

this alloy-disordered system, the intrinsic feature of the nitrogen bound excitonic state is its excitation spectrum and not its emission one, as seen from the fact that the later spectrum is temperature dependent while the former one is not. To derive the electronic structure of the alloy, we have introduced the CPA method and we have estimated, in agreement with experiments, the energy positions, the bandwidths, and the cross sections of the excitation band as a function of composition. We have given arguments showing that the shift between emission and absorption lines is a consequence of the absorption band broadening, the nitrogen bound excitons being able to relax down to the lowest energy configurations.

One of the purposes of this paper consists in showing that the existence of alloy disorder introduces in the luminescence of GaAsP:N new effects in comparison with GaP:N. We have discussed the interest in the ability of the isoelectronic nitrogen impurity as a local probe in the $\text{GaP}_x\text{As}_{1-x}$ matrix to reveal the disorder effect, the band broadening being a direct consequence of the various As-P configurations around the nitrogen atoms. We have also shown that these disorder effects must enter into the whole description of the electronic structure, and that the coherent-potential approximation method, in spite of some approximations, is able to account for these effects. From the theoretical viewpoint, it may be worth emphasizing the relevance of the CPA method in this kind of problems: while up to now, the use of the CPA had been mainly restricted to phonon or to metallic-alloy problems and had yielded essentially the energy position of the alloy states, we have been able to introduce the CPA in the study of the electronic structure of semiconductor alloys and from it to get informations about the linewidth and the cross section of impurity levels.

The qualitative and quantitative explanations we give respectively for the luminescence and excitation mechanisms bring a new insight into the nitrogen-center properties in an alloy such as GaPAs. While Wolford *et al.* developed the study of phonon participations characteristic of optically active centers (nitrogen, selenium) and while Hsu *et al.* and Kleiman *et al.* tried to calculate the bound-state energies in models extended to several sites, all our experimental and theoretical results show the importance of local disorder effects on the electronic properties of nitrogen centers and somewhat deeply modify the understanding of luminescence mechanisms in GaPAs:N alloys. This luminescence band is generated by the radiative recombination of nitrogen bound excitons thermalized to the bottom of the absorption band broadened by alloy disorder. In order to get a better understanding of

these recombination phenomena it would be useful to perform a detailed analysis of energy-transfer mechanisms between the various substates of the excitonic band. We expect these processes to be dependent on the temperature and the nitrogen concentration of the alloy.

This local disorder being specific to alloys, one may expect it to occur in other semiconducting systems. In this respect, it would be worth performing a comprehensive study of the relevant parameters, namely the relative magnitude of the host-alloy potential difference, the relative magnitude and the structure of the defect potential, and the role of the disorder topology (disorder occurring on the first or second neighbors), by studying systems like GaInP:N, or GaAlAs.

ACKNOWLEDGMENTS

Optical experiments were performed at the Max Planck Institut, Stuttgart, in Professor H. J. Queisser's group. We thank Professor H. J. Queisser for his hospitality at the Max Planck Institut, Stuttgart, to one of us (H.M.) and for stimulating discussions during the course of this work. We are grateful to G. Poiblaud of RTC—La Radiotechnique—Compelec, Caen, for providing the samples and to W. Heinz (Stuttgart) for technical assistance in the optical experiments.

APPENDIX

The partitioning scheme proposed by Scifres *et al.*¹⁵ was relying only on considerations of radii in reciprocal space but did not give any attention to the Brillouin-zone geometry. Our partitioning scheme conserves the total volume of the Brillouin zone shown in Fig. 9 and respects the symmetry of the *X* and *L* faces; we assume that the solid angles associated with these faces are equal

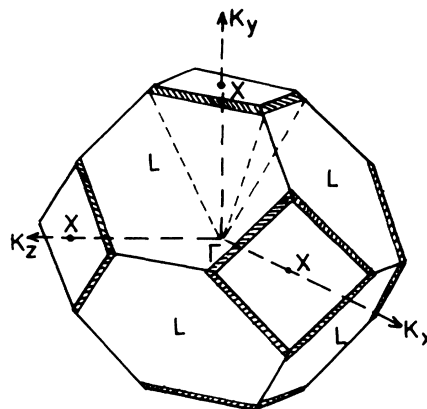


FIG. 9. *X* and *L* partitioning in the first Brillouin zone showing how the *X* zones overlap the *L* faces.

so that the pyramids centered on the X face overlap L faces. Finally, we assume that the volume enclosing the Γ states is bounded by squares and hexagonal faces homothetic to the X and L faces, respectively. The heights of this volume are obtained from the consideration of the schematic band structure of GaAs and GaP given in Ref. 7.

Straightforward geometrical arguments then provide us with the P_α . Using the values of the effective masses in GaAs (Ref. 28) and GaP (Ref. 2) and the band edge positions in these compounds,^{25,26} we are able to estimate the parameters V_α and W_α which are given in Table I.

*Permanent address.

- ¹P. J. Dean, *J. Lumin.* **1**, 398 (1970); R. A. Logan, P. J. Dean, H. G. White, and W. Wiegmann, *J. Appl. Phys.* **42**, 2328 (1971).
²J. Chevallier, H. Mariette, D. Diguët, and G. Poiblaud, *Appl. Phys. Lett.*, **28**, 375 (1976).
³H. Mariette and J. Chevallier, *Solid Stat. Commun.* **29**, 263 (1979).
⁴D. J. Wolford, B. G. Streetman, Shui Lai, and M. V. Klein, *Solid State Commun.* **32**, 51 (1979).
⁵R. J. Nelson, N. Holonyak, Jr., J. J. Coleman, D. Lazarus, W. O. Groves, D. L. Keune, M. G. Craford, D. J. Wolford, and B. G. Streetman, *Phys. Rev. B* **14**, 685 (1976); D. J. Wolford, B. G. Streetman, R. J. Nelson, N. Holonyak, Jr., *Solid State Commun.*, **19**, 741 (1976).
⁶M. Gal, T. Görög, and A. Keresztury, *Solid State Commun.* **21**, 491 (1977).
⁷W. Y. Hsu, J. D. Dow, D. J. Wolford, and B. G. Streetman, *Phys. Rev. B* **16**, 1597 (1977).
⁸G. G. Kleiman and M. Fracastoro-Decker, *Phys. Rev. B* **17**, 924 (1978); **21**, 3478 (1980).
⁹M. Jaros and S. Brand, *J. Phys. C* **12**, 525 (1979).
¹⁰A. B. Chen and A. Sher, *Phys. Rev. Lett.* **40**, 900 (1978).
¹¹E. Cohen and M. D. Sturge, *Phys. Rev. B* **15**, 1039 (1977).
¹²D. J. Wolford, W. Y. Hsu, J. D. Dow, and B. G. Streetman, *J. Lumin.* **18/19**, 863 (1979).
¹³P. J. Wiesner, R. A. Street, and H. D. Wolf, *Phys. Rev. Lett.* **35**, 1366 (1975).

- ¹⁴H. Mariette and J. Chevallier, *J. Appl. Phys.* **48**, 1200 (1977).
¹⁵D. R. Scifres, N. Holonyak, Jr., C. B. Duke, G. G. Kleiman, A. B. Kunz, M. G. Craford, W. O. Groves, and A. H. Herzog, *Phys. Rev. Lett.* **27**, 191 (1971).
¹⁶P. Soven, *Phys. Rev.* **156**, 809 (1967); **178**, 1136 (1969).
¹⁷B. Velicky, S. Kirpatrick, and H. Ehrenreich, *Phys. Rev.* **175**, 747 (1968).
¹⁸For a review see R. J. Elliott, J. A. Krumhansl, and P. L. Leath, *Rev. Mod. Phys.* **46**, 465 (1974).
¹⁹J. C. Campbell, N. Holonyak, Jr., M. G. Craford, and D. L. Keune, *J. Appl. Phys.* **45**, 4543 (1974).
²⁰B. Velicky, *Phys. Rev.* **184**, 614 (1969); B. Velicky and K. Levin, *Phys. Rev. B* **2**, 983 (1970).
²¹W. H. Butler, *Phys. Rev. B* **8**, 4499 (1973).
²²C. T. White and E. N. Economou, *Phys. Rev. B* **15**, 3742 (1977).
²³F. Brouers, M. Cyrot, and F. Cyrot-Lackman, *Phys. Rev. B* **7**, 4370 (1973).
²⁴N. Shevchik, J. Tejada, and M. Cardona, *Phys. Rev. B* **9**, 2627 (1974).
²⁵A. Onton and L. M. Foster, *J. Appl. Phys.* **43**, 5084 (1972).
²⁶H. Mathieu, P. Merle, and E. L. Ameziane, *Phys. Rev. B* **15**, 2048 (1977).
²⁷D. G. Thomas and J. J. Hopfield, *Phys. Rev. B* **150**, 680 (1966).
²⁸D. E. Aspnes, *Phys. Rev. B* **14**, 5331 (1976).
²⁹H. P. Hjalmarson, P. Vogl, D. J. Wolford, and J. D. Dow, *Phys. Rev. Lett.* **44**, 810 (1980).